Journal of
Nanoelectronics and Optoelectronics
Vol. 3, 44–54, 2008

REVIEW

Near-Field Optical Transducer for Heat-Assisted Magnetic Recording for Beyond-10-Tbit/in^2 Densities

R. Ikkawi[1,*], N. Amos[1], A. Lavrenov[1], A. Krichevsky[1], D. Teweldebrhan[2], S. Ghosh[2], A. A. Balandin[2], D. Litvinov[3], and S. Khizroev[4]

[1] *Center for 3D Electronics, Department of Electrical Engineering, University of California – Riverside, Riverside, CA 92521, USA*
[2] *Nano-Device Laboratory, Department of Electrical Engineering, University of California – Riverside, Riverside, CA 92521, USA*
[3] *Center for Nanomagnetic Systems, Department of Electrical and Computer Engineering, University of Houston, Houston, Texas 77204, USA*
[4] *Department of Electrical Engineering, University of California – Riverside, Riverside, CA 92521, USA*

Continuous device downscaling, growing integration densities of the nanoscale electronics and development of alternative information processing paradigms, such as spintronics and quantum computing, call for drastic increase in the data storage capacity. In this paper we review our recent results for the design, fabrication and characterization of the near-field optical transducer for heat-assisted magnetic recording for beyond the 10-Tbit/in^2 densities. In order to record information, the heat-assisted magnetic recording system uses not only magnetic but also thermal energy. For this reason the recording media with the substantially higher anisotropy could be utilized to achieve the ultra-high recording densities. In this review, we provide details of the design of the near-field transducer capable of delivering over 50 μW power into a spot with the diameter of 30 nm. Heat-assisted magnetic recording and spin-based information processing require accurate thermal management of magnetic thin films. Here we report the results of our preliminary investigation of thermal transport in Pd/CoPd/Pd magnetic multilayers with the thickness of individual layers in the nanometer range.

Keywords: Heat Assisted Magnetic Recording, Focused Ion Beam, Near-Field Scanning Optical Microscopy, Heat Diffusion.

CONTENTS

*Author to whom correspondence should be addressed.

1. INTRODUCTION

1.1. Heat-Assisted Magnetic Recording

Recently it became clear that the conventional magnetic recording schemes are coming to their end because of the superparamagnetic limit.[1] Heat-assisted magnetic recording (HAMR) may have potential to extend the data densities to 10 Terabit/in^2.[2–5] In order to record information, HAMR will use not only magnetic but also thermal energy. Therefore, a recording media with substantially higher anisotropy could be utilized. In one of the proposed implementations, a laser beam in the near field, co-aligned with the recording field, heats up a local region to the temperature close to the Curie point. The key challenge in this implementation is to develop a near-field transducer capable of delivering over 50 μW into a spot diameter of 30 nm. The traditional fiber schemes are barely capable of producing 10 nW. To resolve this issue, a laser diode could be placed with the emitting edge only a few nanometers

 1555-130X/2008/3/044/011 doi:10.1166/jno.2008.007

away from the recording media. The light can propagate through a nano-aperture on the surface of an aluminum-coated emitting edge.

In this paper we present an overview of our recent experimental studies focused on recording characteristics of the various near-field transducers fabricated using the focused ion beam (FIB) technology.[6] In order to count the number of photons emitted in the near field we have implemented a special near-field scanning optical microscopy (NSOM) system (see Fig. 1). Our experimental results

Rabee Ikkawi received his B.S. and M.S. in Electrical and Computer Engineering from the Florida International University (FIU), Miami, FL, in 2005 and 2006, respectively. Currently, he is a Ph.D. candidate at the University of California – Riverside (UCR). He is expected to recieve his Ph.D. in Electrical Engineering from UCR in Spring 2008. The focus of his research is the development of near-field optical systems for next-generation information storage applications, especially heat-assisted magnetic recording and protein-based memory. He has authored over ten publications in refereed journals. He is the recipient of 2005 Center for Nanoscale Magnetic Devices (CNMD) Best Graduate Student Award. In 2007, he was awarded an extended research internship at Western Digital Corporation, San Jose, California. He is credited for transferring the nanolasing technology he developed at UCR to advance the state of HAMR development at Western Digital. His groundbreaking experiment to demonstrate the feasibility of using nanolasers to deliver relatively large amount of light power into a 30-nm spot size was presented in the December 2007 issue of MIT Technology Review.

Nissim Amos received his B.S. and M.S. in Electrical Engineering from the Florida International University (FIU) in 2005 and 2006, respectively. Currently, he is a Ph.D. candidate at the University of California – Riverside (UCR). In 2005, he was the only student out of several hundred graduating students at FIU who graduated with the highest GPA of 4.0. He is expected to graduate with Ph.D. in Electrical Engineering from UCR in Spring 2008. The focus of his research is the development of multilevel three-dimensional (3D) magnetic recording. In December 2004, he was awarded a highly selective Undergraduate Student Fellowship by US Air Force Office of Scientific Research (AFOSR). He is the recipient of 2005 Center for Nanoscale Magnetic Devices (CNMD) Best Graduate Student Award. In summer 2007, as a graduate intern at Seagate Research, Nissim was the first graduate student who transferred the technology of multilevel recording to the industry.

Andrey Lavrenov received his M.S. degree in Quantum Electronics from the Moscow Institute of Physics and Technology (MIPT), Moscow, Russia, and Ph.D. in Electrical and Computer Engineering from the Florida International University (FIU), Miami, Florida. He is currently a post-doctoral fellow at the Department of Electrical Engineering, University of California – Riverside (UCR). His research interests involve nanomagnetic systems, magnetic recording, and focused ion beam (FIB) based nanofabrication.

Alexander Krichevsky received his Ph.D. and M.S. degrees in Physics from the University of Alberta under supervision of Professor Mark Freeman and Weizman Institute of Science, respectively. His Ph.D. study was devoted to the ultra-fast measurements and characterization of magnetization reversal in ferromagnetic microstructures using the Time Resolved Scanning Kerr Microscopy (TR-SKM) technique. His research focused on the fabrication and characterization of prototype Magnetic Random Access Memory (MRAM) elements. Alexander continued his work as a Research Scientist and Postdoctoral Fellow in the Naval Research Laboratory and the George Washington University in Washington D.C. with Dr. Mark Johnson. This research was also focused on the transport properties of a novel, hybrid ferromagnetic-semiconductor prototype MRAM elements. Since October 2006, Alexander has joined Professor Khizroev's group in the University of California – Riverside (UCR) where he continued to work on the design and characterization of the magnetic memory elements in multilayer assembly.

Desalegne B. Teweldebrhan received his B.S. in Physics with a minor in Chemistry from the University of California – Riverside (UCR) in 2007. He has worked as a Research Assistant in the Department of Physics and Astronomy at UCR from 2005 to 2007 specializing in the high temperature—ultra high vacuum epitaxial growth. Currently, he is Ph.D. graduate student in the Department of Electrical Engineering at UCR. He is a member of the Nano-Device Laboratory (NDL) under the advisory of Professor Alexander A. Balandin. His current research interests include thermal transport measurements in nanostructured materials, graphene characterization and graphene-based electronic devices. He has been awarded the Outstanding Undergraduate Researcher Award by the Department of Physics and Astronomy. He was also awarded a prestigious Bridge to Doctorate Fellowship in 2007. He is a student-member of the FCRP Center on Functional Engineered Nano Architectonics at UCLA.

Suchismita Ghosh received her B.S. degree in Electrical Engineering from Jadavpur University, Calcutta, India in 2003. She received her M.S. degree in Electrical Engineering from University of California – Riverside (UCR) in 2006 with a specialization in Nano Materials, Devices and Circuits. During the period 2003–2004 she worked as a design engineer in Crompton Greaves, India. Since Fall 2005 she has been working on her Ph.D. degree under the guidance of Professor Alexander A. Balandin at the Nano-Device Laboratory at UCR. Her current research revolves around the characterization of the nanostructured materials and thermal management of the nanoscale devices and circuits. Along with the experimental techniques for measuring materials thermal properties, modeling and theoretical study of the effects of the acoustic phonon confinement on the lattice thermal conductivity is also an important part of her doctoral research. In 2007 she won the 3rd place award in the prestigious national competition organized by The Society of Women Engineers and sponsored by IBM and Rockwell corporations for her research poster presentation on the measurement of the thermal conductivity of the nanocrystalline diamond films by the transient plane source technique. She is a student-member of the FCRP Center on Functional Engineered Nano Architectonics at UCLA.

Alexander A. Balandin received his B.S. (1989) and M.S. (1991) degrees *Summa Cum Laude* in Applied Physics & Mathematics from the Moscow Institute of Physics & Technology (MIPT), Russia. He received his second M.S. (1995) and Ph.D. (1997) degrees in Electrical Engineering from the University of Notre Dame, USA. He worked as a Research Engineer in the Device Research Laboratory (DRL) at the Electrical Engineering Department, University of California – Los Angeles (UCLA) from 1997 to 1999. In 1999, he joined the Department of Electrical Engineering, University of California – Riverside (UCR), where he is a Professor of Electrical Engineering. He leads the Nano-Device Laboratory (NDL), which he organized in 2000. In 2005 he was a Visiting Professor at the Engineering Department, University of Cambridge, UK. In 2007 he became a Founding Chair of the Materials Science and Engineering (MS&E) Program at UCR. Professor Balandin's research interests are in the area of electronic materials, nanostructures and devices. He carries out both experimental and theoretical/modeling research. He made significant contributions to understanding the phonon and exciton confinement effects in semiconductor nanostructures and investigation of the thermal transport and electronic noise phenomena in the wide band-gap semiconductors and devices. The current topics of research in his group include graphene nanometrology; thermal conduction in nanostructured materials; nanostructure-based photovoltaic solar cells; phonon-engineered high-performance electronic devices. His work was recognized by the Office of Naval Research (ONR) Young Investigator Award, National Science Foundation CAREER Award, UC Regents Award, Civil Research and Development Foundation Award and the Merrill Lynch Innovation Award. He is a Fellow of the American Association for the Advancement of Science (AAAS), Senior Member of IEEE, Eta Kappa Nu, Member of APS, MRS and an Associate Scholar of Pembroke College, University of Cambridge, UK. He serves as an Editor-in-Chief of the *Journal of Nanoelectronics and Optoelectronics* (JNO). His research group participates in the work of two national research centers: the DARPA-SRC funded FCRP Center on Functional Engineered Nano Architectonics (FENA) and DARPA-DMEA funded UCR-UCLA-UCSB Center for Nanoscience Innovations for Defense (CNID). The work of his research group has been supported though the grants from NSF, ONR, ARO, NASA, AFOSR, SRC, DARPA, CRDF, UC MICRO, IBM, TRW and Raytheon. More information about his research can be found at http://ndl.ee.ucr.edu/.

Dmitri Litvinov received B.S. in Quantum Electronics and Applied Physics from the Moscow Institute of Physics and Technology (MIPT), M.S. in Physics from the University of Miami, and Ph.D. in Applied Physics from the University of Michigan, Ann Arbor, in 1992, 1993, and 1999, respectively. He is a tenured Associate Professor at the department of Electrical and Computer Engineering of the University of Houston (UH), Houston, Texas. Before joining UH in 2003, he had been employed as a research staff member with Seagate Research for over 4 years. He has over 25 granted and 9 pending and 105 provisional patents with Seagate. He has authored/co-authored over 55 refereed papers and 4 books and book chapter. He has served as a Guest Editor for *Nanotechnology* and *IEEE Transactions on Magnetics*. The current research focus is in the sub-area of Nanotechnology dedicated to the development of next generation information storage and memory devices including magnetic, magneto-optical, and protein-based systems. He is a co-founder and co-organizer of IEEE conference on Nanoscale Devices and System Integration (NDSI) and North American Perpendicular Magnetic Recording Conference (NAPMRC). He is a Senior Member of IEEE.

Sakhrat Khizroev received B.S. in Quantum Electronics and Applied Physics from the Moscow Institute of Physics and Technology (MIPT), M.S. in Physics from the University of Miami, and Ph.D. in Electrical and Computer Engineering from Carnegie Mellon University (CMU) in 1992, 1994, and 1999, respectively. He is a tenured Associate Professor at the Department of Electrical Engineering, University of California – Riverside (UCR). From 2003 to 2006, he was a tenured faculty at the Florida International University (FIU) where he founded and directed the Center for Nanoscale Magnetic Devices. Before joining FIU, he had been employed as a research staff member with the Seagate Research and as a doctoral intern with the IBM Almaden Research Center. He has over 26 granted and 9 pending and 110 provisional patents with IBM, Seagate, CMU, FIU, and UCR. He has authored/co-authored over 70 refereed papers and 4 books and book chapters. He has served as Associate Editor for *IEEE Transactions on Nanotechnology* and a Guest Editor for *Nanotechnology* and *IEEE Transactions on Magnetics*. His current research focus is in the broad area of multilevel electronics and nanomagnetic devices. He is a co-founder and co-organizer of IEEE conference on Nanoscale Devices and System Integration (NDSI) and North American Perpendicular Magnetic Recording Conference (NAPMRC). He is a Senior Member of IEEE.

indicate that the FIB-fabricated transducers could deliver power of over 100 nW into a 35-nm spot. Heat assisted magnetic recording requires precise control of the heat propagation in the recording medium and accurate thermal management of the whole system. In this paper we address the thermal management issues and present preliminary results of the thermal conductivity measurements using the nano-flash technique.

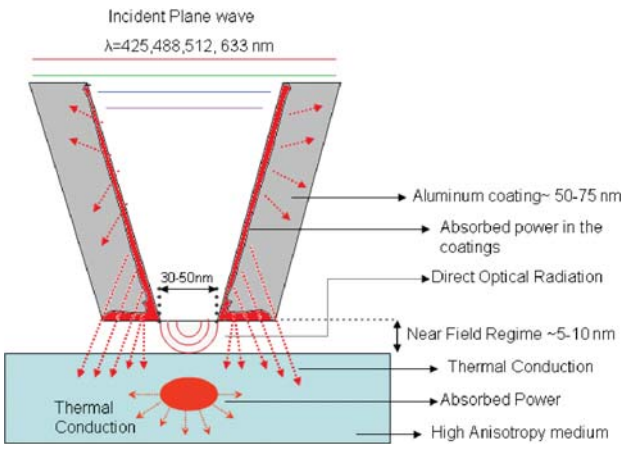

Fig. 1. Schematic of the cross-section of SNOM probe depicting the heat sources and thermal conduction paths.

1.2. Near-Field Optical Systems for Ultra-High Data Storage

Achieving the high spatial resolution beyond the diffraction limit was first proposed in 1928 by utilizing the optical near field of small apertures in metallic plates.[7–9] Since then, researchers have made tremendous efforts to apply the near-field optical systems for the ultrahigh density data storage,[10–12] ultrahigh resolution lithography,[13] protein based memory[14, 15] or other applications that require highly localized heating of the sample surface. In the field of data storage, HAMR is believed to be a promising next-generation technology that could truly benefit from the near-field implementation. However, the development of HAMR and the other applications could be hindered if the design does not overcome a critical problem: inadequately low power transmission efficiencies through the sub-wavelength apertures.

The most widely used near-field probe is a metal-coated tapered optical fiber which suffers from the extremely

low power transmission: $\sim 10^{-6}$ for a 100-nm aperture size.[16] Several probe ideas to circumvent the mode cut-off problem were proposed. They include the bow-tie antenna, I-shaped, C-shaped, and L-shaped apertures[17–19] where the last two revealed four to six orders of magnitude increase in the power throughput as compared to the conventional square apertures and fiber-based probes (see Fig. 1), respectively.

The proposed HAMR concept enables the use of the smallest possible thermally stable grains, irrespective of the ultra-large intrinsic anisotropy. It exploits the substantial drop of the medium's coercivity when the disk temperature is elevated close to its Curie level.[20–22] In the next section we present our design of the heating element based on the ultra-high-efficiency near-field optics suitable for extending the area densities beyond 10 Tbit/in^2. We specifically focus on the experimental and theoretical study of the issues associated with the localization of an adequate amount of heat into a spot size smaller than 60 nm on the recording media.

2. DESIGN OF HEAT-ASSISTED MAGNETIC RECORDING SYSTEM

It has been estimated that for HAMR systems to record on ultra-high anisotropy media such as, for example, FePt—L10-based and others,[23] a few hundreds of nano-watts have to be focused into a 50 nm spot. The contribution of both the optical energy and magnetic energy will facilitate recording on this 3 nm grain size medium to conceive one terabit of ultra-stable recorded bits on the square of an inch. Such high power delivery system could be achieved by utilizing the antenna focusing techniques on a metal-coated edge of a high power laser diode placed directly at an air bearing surface (ABS). Among a large number of proposed designs the one, which is particularly promising is the "C" shape aperture, which can not only dodge the diffraction limit by an order of magnitude, but can also provide a high-power throughput sufficient for HAMR recording.[24]

2.1. Modeling Study of Light Focusing by Different Apertures

We have used a finite-element method (FEM) to simulate the light propagation in the near field for the slit structures with different geometrical shapes. The governing Maxwell's equations for a slit structure are divided into the transverse magnetic (TM) and transverse electric (TE) modes. The TM and TE modes correspond to the *s*-polarized light and the *p*-polarized light, respectively. The metallic (Al) film is 120 nm thick with a slit element size varying from $\lambda/20$ to $\lambda/10$. The refractive indices for the glass and the Al metal are 1.5, $1.2+7.26i$, respectively. A sinusoidal wave with a wavelength of 600 nm that can be linearly polarized in the *x*- and *y*-directions is excited from the glass substrate. The area of the simulation domain is ($2.0\ \mu\text{m} \times 3.0\ \mu\text{m}$), so the amplitude and the phase of the focused field do not vary much in the simulation area allowing the incident plane wave approximation. To avoid reflections from the boundaries, absorbing boundary conditions are utilized. The objective of the simulation study is to investigate the dependence of two parameters: transmission power throughput and the intensity near-field distribution in addition to exploring the effects of polarization and shape.

The transmission power throughput is defined as the ratio of the total transmitted power to the total incident power over the aperture area. The total transmitted power is calculated by integrating the Poynting vectors over a surface that completely covers the aperture in the transmission region. The total incident power over the aperture's area is calculated by multiplying the incident power flux by the physical area of the aperture. This parameter prevails over transmission efficiency, which is defined as the ratio of the total transmitted power to the total incident power since the difference of the various aperture areas have already been accounted for. The results of the simulation for the intensity distribution and coupled power of the TE mode (*p*-polarized) and TM mode (*s*-polarized) for all the proposed shapes are shown in Figure 2.

Our modeling and numerical simulation study reveal the following results.

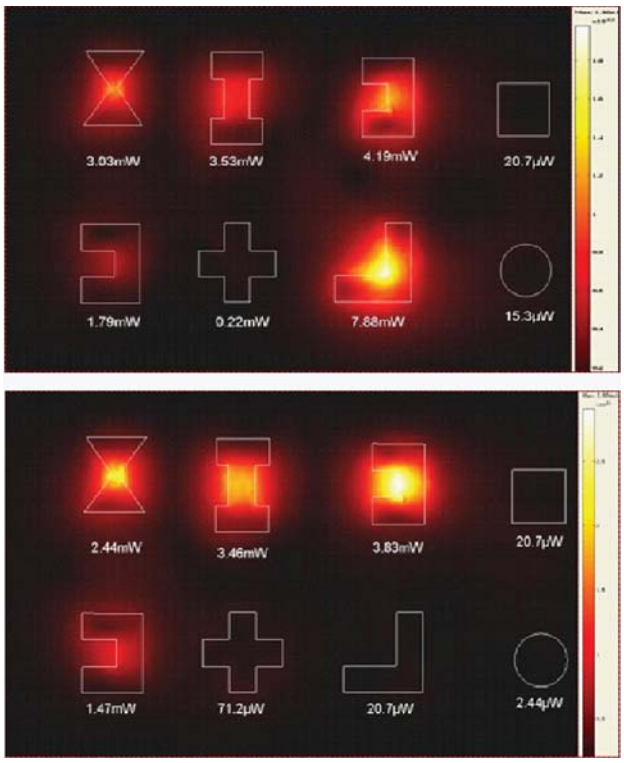

Fig. 2. Near field intensity distribution for apertures of various shapes illuminated with TE (upper panel) and TM (lower panel) polarized light.

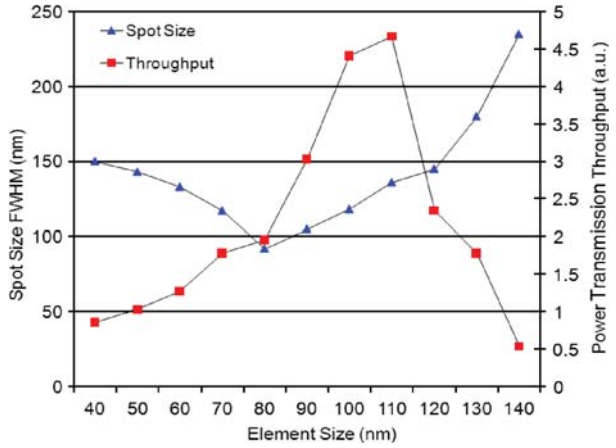

Fig. 3. Power transmission throughput and spot size FWHM as a function of the "C" shape aperture element size.

(i) The power throughput in an order of magnitude higher when the "L" shape aperture is illuminated with TE polarized light as compared to TM polarized light.
(ii) The bow-tie antenna demonstrated the optimum focusing but not the highest transmission efficiency.
(iii) The "C" apertures demonstrated a superlative combination between focusing capability and transmission efficiency as compared to the bowtie and L shape antenna. The "C" shape aperture with a 70 nm element size can yield a few μWs of power focused into a spot with the full width at half maximum (FWHM) of 95 nm.

2.2. Optimization of the "C" Shape Aperture Parameters

Based on the results of our modeling study, we conducted subsequent analysis for the "C" shape aperture only focusing on its throughput, near-field intensity distribution and polarization effect. The data presented in Figure 3 verify that the "C" shape aperture with an element size of 70–80 nm yields the smallest spot size (FWHM of 90 nm) with transmission power throughput close to 200%. It is then evident that power throughput can increase to more

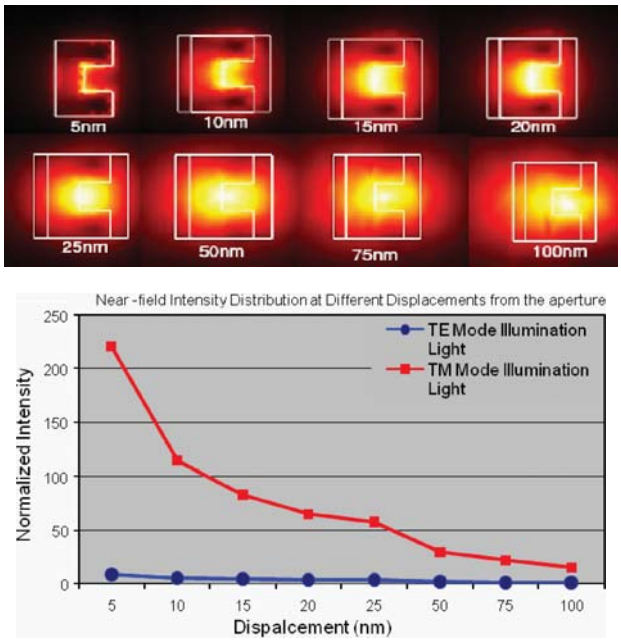

Fig. 4. Auto-scaled intensity distribution at different distances for the TM polarized light (upper panel) and the corresponding peak intensity as a function of distance for the TE and TM polarized light.

than 400% when an aperture with a 100–110 nm element size is utilized, but under the constraint of an increased spot size that can reach a FWHM of 150 nm. For subwavelength apertures in resonance, the power transmission cross section can be larger than the aperture area; therefore the PT value can be larger than 1. The law of energy conservation only requires that the power transmission cross section be smaller than the illumination area, but not necessarily smaller than the aperture area. For subwavelength apertures, the illumination area, which is typically at the diffraction limit, is much larger than the aperture area.

In an effort to determine the optimum head-media separation, the intensity distribution was monitored at different distances in the near-field regime of the aperture. It was observed that the near-field intensity distribution changes

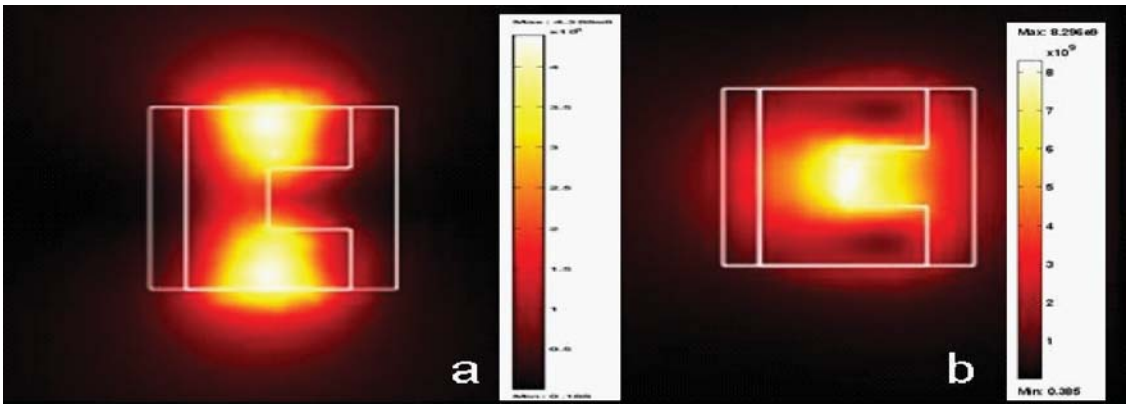

Fig. 5. Near-field intensity distribution for (a) TE and (b) TM polarized incident light.

REVIEW

significantly along its propagation. At the very close distance from the aperture, two hot spots start showing at the edges of the aperture perpendicular to the polarization direction of the incident light. As the distance increases, these hot spots merge into one of approximately 20–25 nm, and to a spot about twice the size of the aperture at 100 nm (see Fig. 4). The date presented in Figure 4 also explains the decay of the near-field peak intensity away from the aperture. It could be noted that the peak intensity drops by a factor of $\sim$10 between 5 and 100 nm. Away from the 100-nm plane, the peak intensity decays as $\sim 1/z^2$

The polarization state of the incident light was found to be another critical factor that substantially affects the localization of the heat in the recording media. The light beam interaction with media leads to depolarization, which results in components with the polarizations different from the polarization of the incident light. This can be interrelated to the abrupt changes in the boundary conditions and the sub-wavelength inference. As follows from our study the sides perpendicular to the polarization direction have a stronger control over the intensity distribution. Various components can also interact with each other and the resonance interference will result in the local field enhancement. Figure 5 profiles the intensity as measured in the near-field for the two incident wave polarizations, TE and TM, respectively.

3. FOCUSED ION BEAM FABRICATION

A 120-nm thick aluminum film is firstly deposited on the glass window of a laser diode via the electron beam vapor deposition. A novel technique will be utilized in future work to conventionally focus light to a few microns spot exploiting classical optics, and subsequently generate the apertures on the optically focused plane. This method is expected to increase throughput by two orders of magnitude as compared to focusing the beam with very high divergence. Secondly, the structure is fabricated using the high resolution focused ion beam (FIB) FEI XP 800 system with 30 keV Ga^+, 1 pA beam current, and Gallium ion flux of 1.3×10^{19} $Ga^+/s \cdot cm^2$. The theoretical minimum beam spot size for this case is 8 nm, and the real spot size is estimated to be 10 nm. The pixel-by-pixel milling method was used to raster patterns with 10 nm step size. The milling was subsequent to the numerically estimated patterns through a personalized developed software codes based on Matlab to minimize the secondary sputtering and redeposition effects. The milling rate was measured with an atomic force microscopy (AFM), and aperture depth was controlled by total milling time that ranged between 5 and 15 seconds, depending on the shape and deepness (see Fig. 6).

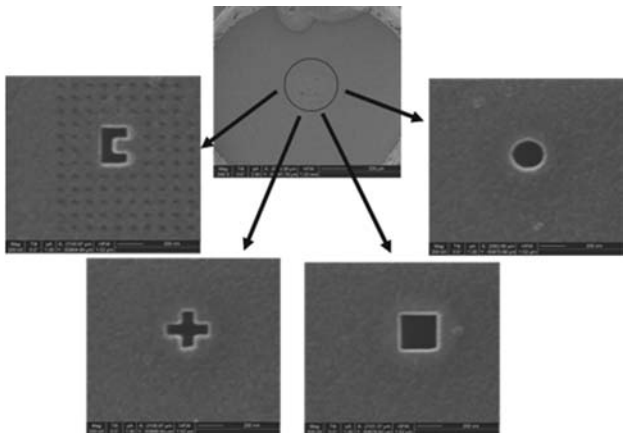

Fig. 6. Apertures of different geometry defined on the emitting edge of a laser diode using FIB fabrication.

4. CHARACTERIZATION OF NSOM PROBES

NSOM makes use of a technique where an aluminum-coated tapered optical fiber probe (see Fig. 1) is placed at a distance (from an imaged sample), which is a fraction of the wavelength of the emitted light. In this particular case, the imaged sample is the emitting edge of a diode laser. The NSOM probe is used to scan the surface of the emitting edge. (see Fig. 6). NSOM probes are used to collect emitted radiation in the near-field to examine the evanescent fields of the waveguides (emission profiles) or as an illumination source to profile surfaces, excite local photoconductivity in the semiconductor, locally heat active devices, etc. In this application NSOM probes provide a nano-sized aperture through which the light is coupled.

4.1. Experimental Setup and Measurement Procedure

The simultaneous shear-force measurements provide an independent measure of the surface topography to maintain a fixed proximity (5–10 nm) between a tip and a sample. The fiber tip is mounted on a quartz tuning-fork and dithered at its resonant frequency with a small piezo-element where any tip-surface interaction quenches the resonance, providing a height measurement with the nanometer resolution (see Fig. 7). The shear-force topography is exploited to correlate various optical profiles with the physical device structure.

In our experiment, the laser diode is mounted face up on a piezo actuated flexure stage and scanned in the xy-plane underneath the probe tip. The collected light is coupled into the optical fiber and transmitted to be analyzed with a photo-multiplier tube (PMT) detector. For input power of 80 μW, output power was measured to be 0.53 μW. Consequently, for 250 mW of input power, assuming linear dependence, over 1.65 mW of power would be focused into a 35-nm radius spot (Fig. 8). This estimation, if validated, counterparts our simulated results.

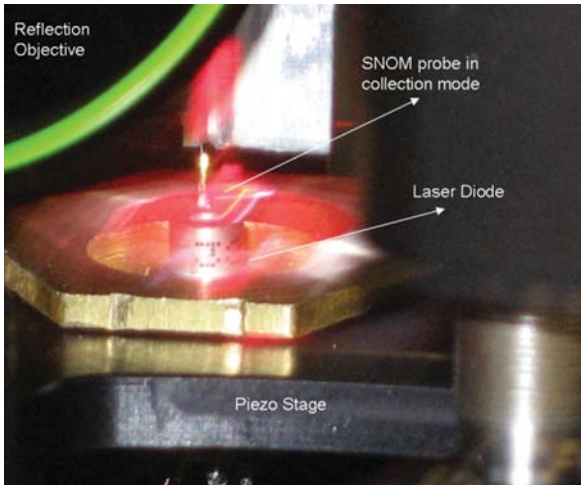

Fig. 7. Experimental setup showing NSOM probe in the collection mode scanning the emitting surface of the coated laser diode.

4.2. Analysis of Light Losses in NSOM Tips

The transmission of light through an NSOM tip is a lossy endeavor. The light in the fiber begins to penetrate the fiber cladding once the core size shrinks (due to the tapered region) to values below a few wavelengths. The light that penetrates the cladding is reflected by the metal coating and thus never reaches the aperture. Due to this process, only 1 out of 10^4–10^5 photons is transmitted through the tip. Increasing the power input to the fiber to compensate for this loss can only be done up to a few mW. If the power input into the fiber is greater than a few mW, heating at the taper becomes inadequately severe and damages the metal/glass interface so that the coating becomes compromised or lost completely in the case of melting (see Fig. 9).[25–29] Therefore, the upper limit to

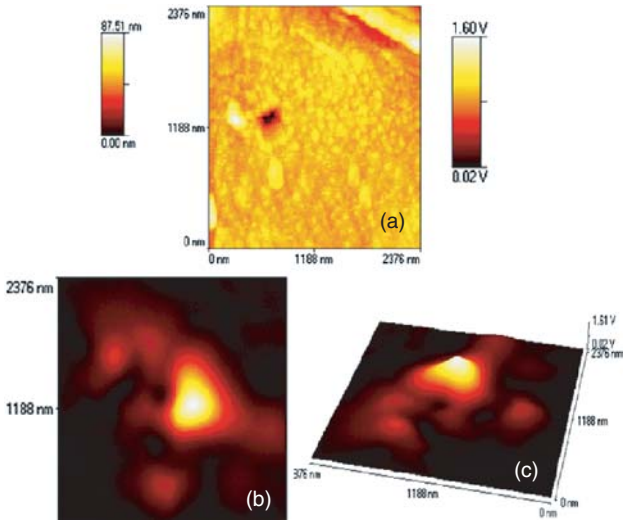

Fig. 8. Topography image of the "C" shape aperture (a) and its corresponding optical image for the collected light in 2D and 3D contour representation, respectively (b and c).

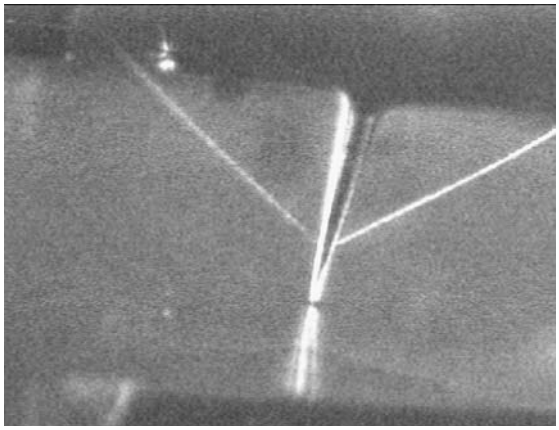

Fig. 9. Snapshot of a melting NSOM probe.

the continuous-wave transmitted power of an NSOM tip is of the order of 100 nW (10^{12} photons/s). In practice, our 100 nm apertures transmit the power of the order of 10 nW (10^{11} photons/s) for an input power of a few mW.[13] This setback limited our collection scanning capabilities at high input powers and restricted the experiments to the lower input power, which NSOM probes can tolerate. To estimate the throughput at the highest input power, we assumed (extrapolated) the same linear dependence of the throughput measured at the lowest input power. The overheating problem discussed above provides an additional motivation of the study of thermal conduction in materials used for HAMR and NSOM tips.

5. THERMAL DIFFUSIVITY OF LAYERED MAGNETIC MEDIA

Heat assisted magnetic recording requires accurate knowledge of the thermal diffusivity α and thermal conductivity K of the materials used as recording medium as well as NSOM probe materials. Transient heat transfer occurs when the temperature distribution or heating source power are changing with time. The fundamental quantity that describes the heat transfer when the system is not at steady-state is the thermal diffusivity α. The thermal diffusivity is related to thermal conductivity through the expression $\alpha = K/\rho C_p$, where ρ is the mass density and C_p is the specific heat of the material. In this section we give an overview of our preliminary results of the thermal characterization. The long term goal of the study of the thermal diffusivity and thermal conductivity described here is to improve the thermal management of the HAMR systems and develop an optimum NSOM design within the thermal constrains.

5.1. Instrumentation for Thermal Diffusivity Measurements

The measurement of the thermal diffusivity of a material is usually performed by rapidly heating one side of

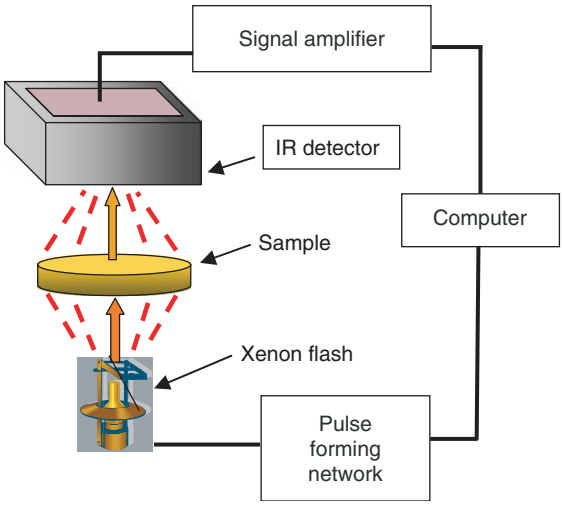

Fig. 10. Schematic of the experimental setup used for measurement of the thermal diffusivity of the magnetic recording media. The "laser flash" type of measurement is based on illumination of the one side of the sample and detecting the temperature rise with IR detector on the opposite side of the sample.

a sample and measuring the temperature rise as a function of time on the opposite side of the sample (see Fig. 10). The recorded time that takes for the heat to travel through the sample and cause the temperature rise on the rear face is used to determine the through-plane diffusivity and calculate the thermal conductivity is the specific heat is know and mass density of the material are known. The Netzsch system, which we used for this study, allowed us to measure the thermal diffusivity values ranging from 0.001 to 10 cm^2/s over a temperature range from 20 °C to 160 °C.

5.2. Measured Thermal Properties of the Substrates and Pd/CoPd/Pd Multilayers

The magnetic recording media, which consists of Pd/CoPd/Pd multilayers, were prepared on the Corning 0211 glass substrates (Zinc Borosilicate). The total thickness of the multilayers varied from approximately 30 to 65 nm. The first essential step was to accurately determine the thermal diffusivity and thermal conductivity of the substrates used. This is required in order to be able to separate the value of the thermal diffusivity for the thin multilayers from that of the substrate. Figure 11 shows the measured thermal diffusivity for the Corning 0211 substrate as a function of temperature. As one can see from this plot the room-temperature value is $\alpha = 4.27 \times 10^{-7}$ m^2/s.

The measured value and temperature dependence are in excellent agreement with the data reported in literature for glass. For example, in Ref. [30], the thermal diffusivity of glass, measured using the photopyroelectric signal spectral analysis, was determined to be $\sim 4.3 \times 10^{-7}$ m^2/s at room temperature. It also manifested decreasing trend as the

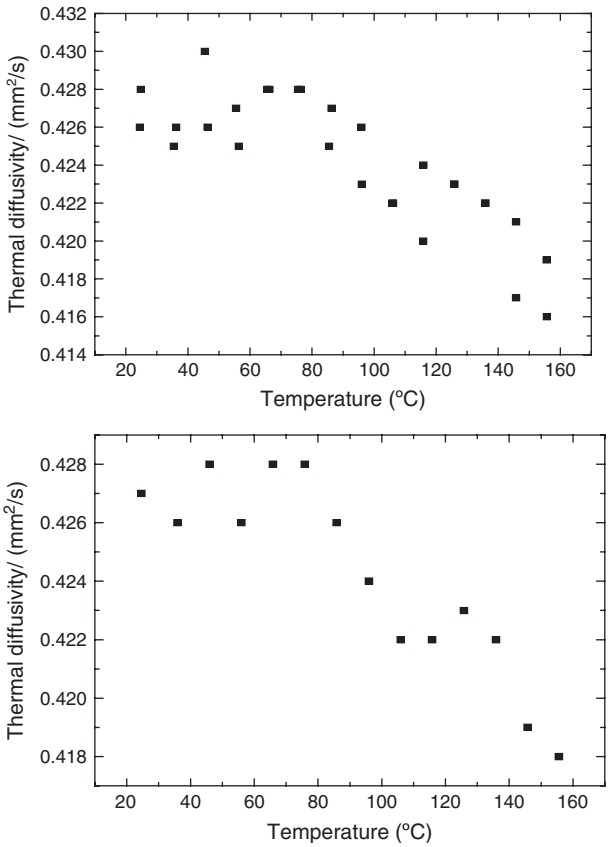

Fig. 11. Measured thermal diffusivity of the substrates used for Pd/CoPd/Pd multilayer deposition: single flash measurements (upper panel) and averaged over many flash measurements (lower panel).

temperature increased from 100 K to 300 K.[30] The agreement with the previously published data indicates that our experimental technique is accurate and fits well the samples of given geometry and material composition. Using a reference sample with the known temperature dependence

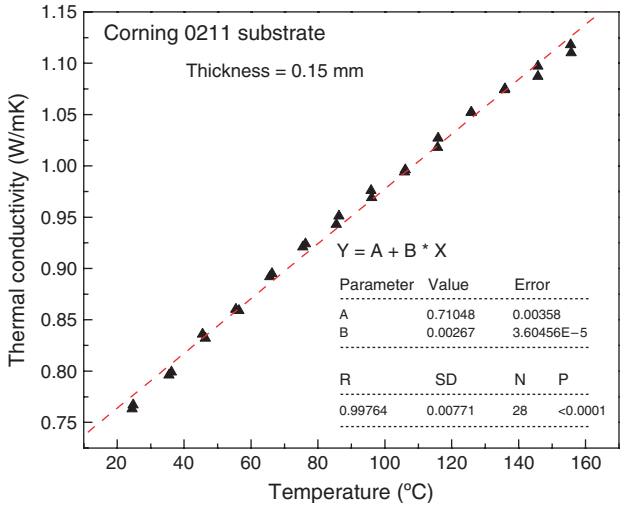

Fig. 12. Measured thermal conductivity of the substrate used for Pd/CoPd/Pd multilayer deposition.

Table I. Measured thermal diffusivity of the Pd/CoPd/Pd multilayers.

Sample type	Pd/CoPd/Pd	Pd/CoPd/Pd/CoPd/Pd	Pd/CoPd/Pd/CoPd/Pd
Thickness (nm)	40	63	63
α, $\times 10^{-6}$ (m^2/s)	10.0	1.1	0.83

of specific heat we were able to determine the thermal conductivity of the Corning 0211 substrates (see Fig. 12). The determined thermal conductivity increases with temperature as typical for the amorphous bulk materials or disordered alloys.[31–33]

After the thermal diffusivity and thermal conductivity values for the substrates have been determined, we focused on the study of Pd/CoPd/Pd multilayers deposited on the Corning 0211 substrates. The thermal diffusivity data for the multilayers revealed much more scatter as compared to the substrate data. Table I gives a summary of the room-temperature results obtained for several samples of different thickness. The diffusivity values were extracted using the adiabatic model with the pulse correction.

Although there have been no previous studies of the thermal diffusivity in such magnetic multilayers it is interesting to compare the obtained results with the previously reported data for Pd and other related alloys. The photoacoustic measurements of the thermal diffusivity of Fe-Co-Al alloys revealed the value of $\sim 11.4 \times 10^{-6}$ m^2/s for $Fe_{0.45}Co_{0.1}Al_{0.45}$.[34] The α value for this alloy was much smaller than the values of the constituent elements, which are 22.7×10^{-6}, 26.8×10^{-6}, and 97.9×10^{-6} m^2/s for Fe, Co and Al, respectively.[34] In another study the room-temperature thermal diffusivity of the Ag-Pd alloys was found to be in the range from 10.8×10^{-6} to 23.1×10^{-6} m^2/s, which was also smaller than the thermal diffusivity of pure Pd of 24.7×10^{-6} m^2/s.[35]

The data, which we measured for the Pd/CoPd/Pd multilayers is consistent with the previous studies of alloys containing Pd and Co. We also observed a decrease in the thermal diffusivity of the multilayers as compared to the thermal diffusivity of Pd ($\alpha = 24.7 \times 10^{-6}$ m^2/s) and Co ($\alpha = 26.8 \times 10^{-6}$ m^2/s) metals. There are two possible effects, which lead to the thermal diffusivity and thermal conductivity reduction. It is well known that heat in metals and alloys is carried by both electrons and acoustic phonons.[33] The increase acoustic phonon scattering in alloys can result in substantial reduction of the phonon thermal conductivity as was found for many materials.[36] Electrons can also be scattered by the alloy disorder with corresponding decrease in thermal conductivity. In addition, the reduction of the thermal diffusivity can be the result of the thermal boundary resistance (TBR) also referred to as Kapitza resistance.[37] The Kapitza resistance at the interface between two solid materials can be rather large even at room temperature.[38] The fact that the thermal diffusivity for the samples with the 63-nm thickness (which have more different layers) was stronger than that for the samples with 40-nm thickness supports an assumption about strong TBR effect.

Our thermal study revealed that the thermal properties of the nanometer scale multilayers are different from the thermal properties of constituent elements and conventional random PdCo alloys. Even further deviation in properties is expected as the individual layer thickness decreases further. In this case, one may expect the acoustic phonon confinement effects[39] and altered electron–phonon interaction. The latter deserves a separate study. The accurate values of the thermal diffusivity and thermal conductivity can be used in the thermal design optimization of the layered magnetic recording medium for the HAMR systems considered in this paper, multilevel three-dimensional nanomagnetic recording media[40–41] and spin logic circuits implemented on the basis of Ni-Fe alloy thin films on semi-insulating substrates.[42]

6. SUMMARY

The various nanoapertures with different geometries were fabricated on the emitting edge of commercial laser diodes using a focused ion beam system. The geometries of the apertures were selected subsequent to the numerical analysis focused on the ultrahigh light transmission through a "C"-shaped nanoaperture. A state-of-the-art NSOM system was utilized to scan the apertures in the collection mode to evaluate the near field performance of the investigated apertures. A 30-nm-radius spot with the estimated power reaching more than one hundred of nanowatts was detected for a "C" aperture with 70–80 nm element size. The limitations for the high power near-field detection have been discussed. The results of the preliminary investigation of the thermal diffusivity of the layered magnetic recording medium using the "laser flash" technique have also been reported. The thermal management of the nanometer scale magnetic recording medium is crucial for the development of the heat-assisted magnetic recording systems. The knowledge of heat transport in thin magnetic films is also important for the implementation of the spin-based logic circuits.

Acknowledgments: The work in the Center for 3D Electronics (S. Khizroev) has been partially supported by four grants from the National Science Foundation (NSF), ECS-0401297, ECS-0508218, ECS-0404308, and IIP-0712445, respectively, two grants from U.S. Air Force Office of Scientific Research (AFOSR), FA9550-04-1-0446 and FA9550-05-1-0232, respectively, and one grant co-sponsored by the Defence MicroElectronics

Activity (DMEA) and Office of Naval Research (ONR), ONR/DMEA-H94003-07-2-0703. The work in the Nano-Device Laboratory (A. A. Balandin) has been supported, in part, by DARPA-SRC through the FCRP Center on Functional Engineered Nano Architectonics (FENA) and DARPA-DMEA through the UCR-UCLA-UCSB Center for Nanoscience Innovations for Defense (CNID). The authors acknowledge the help with the equipment installation and measurements of other NDL group members (http://www.ndl.ee.ucr.edu).

References and Notes

1. D. Weller and A. Moser, *IEEE Transactions on Magnetics* 35, 6 **(1999)**.
2. K. Matsumoto, A. Inomata, and S. Hasegawa, *Fujitsu Sci. Tech. J.* 42, 158 **(2006)**.
3. R. Rottmayer, S. Batra, D. Buechel, W. Challener, J. Hohlfeld, Y. Kubota, and L. Li, *IEEE Transactions on Magnetics* 42, 10 **(2006)**.
4. H. Katayama, M. Hamamoto, J. Sato, Y. Murakami, and K. Kojima. *IEEE Transactions on Magnetics* 36, 1 **(2000)**.
5. T. McDaniel and W. Challener, *IEEE Transactions on Magnetics* 39, 1972 **(2003)**.
6. S. Khizroev and D. Litvinov, *Review in Nanotechnology* 14, R7 **(2004)**.
7. E. H. Synge, *Mag. J. Sci.* 6, 356 **(1928)**.
8. J. Lin, *Journal of the Optical Society of America* 62, 8 **(1972)**.
9. E. Betzig, A. Harootunian, A. Lewis, and M. Isaacson, *Appl. Opt.* 25, 15 **(1986)**.
10. H. Katayama, *J. Magn. Soc. Jpn.* 23, 233 **(1999)**.
11. E. Betzig, J. K. Trautman, R. Wolfe, E. M. Gyorgy, and P. L. Finn, *Appl. Phys. Lett.* 61, 142 **(1992)**.
12. X. Shi, L. Hesselink, and R. Thornton, *Jpn. J. Appl. Phys.* 41, 1632 **(2002)**.
13. S. Kämmer, P. Tang, and V. Gorbunov, Performing Near-Field Scanning Optical Lithography with the Aurora NSOM, Veeco Instruments, Inc., Sunnyvale **(2003)**.
14. V. Renugopalakrishnan, S. Khizroev, L. Lindvold, P. Li, and H. Anand, *International Conference on Nanoscience and Nanotechnology, 2006. ICONN '06.* IEEE **(2006)**, pp. 228–230.
15. R. R. Birge, *Scientific American* 3, 90 **(1995)**.
16. G. A. Valaskovic, M. Holton, and G. H. Morrison, *Appl. Opt.* 34, 1215 **(1995)**.
17. F. Chen, D. Stancil, and T. Schlesinger, *J. Appl. Phys.* 93, 10 **(2003)**.
18. X. Shi and L. Hesselink, *Opt. Lett.* 28, 15 **(2003)**.
19. J. Xu, T. Xu, J. Wang, and Q. Tian, *Optical Engineering* 44, 018001 **(2005)**.
20. T. Devolder, *Physical Review* 62, 9 **(2000)**.
21. A. Chtchelkanova, S. Wolf, and Y. Idzerda, Magnetic Interactions and Spin Transport, Kluwer Academic/Plenum Publishers, NY **(2003)**.
22. V. Franco and A. Conde, *J. Magn. Magn. Mater.* 215–216, 400 **(2004)**.
23. B. Rellinghaus, S. Stappert, M. Acet, and E. Wassermann, *J. Magn. Magn. Mater.* 266, 142 **(2003)**.
24. R. Ikkawi, N. Amos, A. Krichevsky, R. Chomko, D. Litvinov, and S. Khizroev, *Appl. Phys. Lett.* 91, 153115 **(2007)**.
25. B. I. Yakobson, A. LaRosa, H. D. Hallen, and M. A. Paesler, *Ultramicroscopy* 59, 334 **(1995)**.
26. A. H. La Rosa and H. D. Hallen, *J. Appl. Opt.* 41, 2015 **(2002)**.
27. J. Kann and T. Milster, *Appl. Opt.* 36, 5951 **(1997)**.
28. P. G. Gucciardi, S. Patanè, A. Ambrosio, and M. Allegrini, *Appl. Phys. Lett.* 86, 203109 **(2005)**.
29. A. H. La Rosa, B. I. Yakobson, and H. D. Hallen, *Appl. Phys. Lett.* 67, 2597 **(1995)**.
30. B. Bonno, J. L. Laporte, and R. Tascon d'Leon, *Rev. Sci. Instrum.* 67, 3616 **(1996)**.
31. M. Shamsa, W. L. Liu, A. A. Balandin, C. Casiraghi, W. I. Milne, and A. C. Ferrari, *Appl. Phys. Lett.* 89, 161921 **(2006)**.
32. A. A. Balandin, Thermal conductivity of semiconductor nanostructures, Encyclopedia of Nanoscience and Nanotechnology, edited by H. S. Nalwa, ASP, Los Angeles **(2004)**, pp. 425–445.
33. M. Shamsa, W. L. Liu, A. A. Balandin, and J. L. Liu, *Appl. Phys. Lett.* 87, 202105 **(2005)**.
34. K. A. Azez, *J. Alloys and Compounds* 424, 4 **(2006)**.
35. K. Miyanaga, Y. Kayano, and H. Inoue, *IEICE Trans. Electron.* E90-C, 1405 **(2007)**.
36. W. L. Liu and A. A. Balandin, *J. Appl. Phys.* 97, 073710 **(2005)**.
37. P. L. Kapitza, *Journal of Physics (Moscow)* 4, 181 **(1941)**.
38. K. Filippov and A. A. Balandin, *J. Nitride Semiconductor Research* 8, 4 **(2003)**.
39. A. Balandin and K. L. Wang, *Phys. Rev. B* 58, 1544 **(1998)**; A. Khitun, A. Balandin, J. L. Liu, and K. L. Wang, *J. Appl. Phys.* 88, 696 **(2000)**; E. P. Pokatilov, D. Nika, and A. A. Balandin, *J. Appl. Phys.* 95, 5626 **(2004)**.
40. N. Amos, R. Ikkawi, A. Krichevsky, R. Fernandez, E. Stefanescu, I. Dumer, D. Litvinov, and S. Khizroev, *J. Nanoelectron. Optoelectron.* 2, 257 **(2007)**.
41. N. Amos, A. Lavrenov, R. Ikkawi, P. Gomez, F. Candocia, R. Chomko, D. Litvinov, and S. Khizroev, *J. Nanoelectron. Optoelectron.* 2, 202 **(2007)**.
42. A. Khitun and K. L. Wang, *J. Nanoelectron. Optoelectron.* 1, 71 **(2006)**.

Received: 21 November 2007. Revised/Accepted: 17 December 2007.

REVIEW